



This is a repository copy of *The influence of feed rate on process damping in milling: Modelling and experiments.*

White Rose Research Online URL for this paper:
<http://eprints.whiterose.ac.uk/11062/>

Article:

Sims, N.D. and Turner, S. (2011) The influence of feed rate on process damping in milling: Modelling and experiments. Proceedings of the Institution of Mechanical Engineers, Part B, Journal of Engineering Manufacture, 225 (6). pp. 799-810. ISSN 0954-4054

doi: 10.1243/09544054JEM2141

Reuse

Unless indicated otherwise, fulltext items are protected by copyright with all rights reserved. The copyright exception in section 29 of the Copyright, Designs and Patents Act 1988 allows the making of a single copy solely for the purpose of non-commercial research or private study within the limits of fair dealing. The publisher or other rights-holder may allow further reproduction and re-use of this version - refer to the White Rose Research Online record for this item. Where records identify the publisher as the copyright holder, users can verify any specific terms of use on the publisher's website.

Takedown

If you consider content in White Rose Research Online to be in breach of UK law, please notify us by emailing eprints@whiterose.ac.uk including the URL of the record and the reason for the withdrawal request.



eprints@whiterose.ac.uk
<https://eprints.whiterose.ac.uk/>

Proceedings of the Institution of Mechanical Engineers, Part B: Journal of Engineering Manufacture

<http://pib.sagepub.com/>

The influence of feed rate on process damping in milling: modelling and experiments

N D Sims and M S Turner

Proceedings of the Institution of Mechanical Engineers, Part B: Journal of Engineering Manufacture 2011 225: 799

DOI: 10.1243/09544054JEM2141

The online version of this article can be found at:

<http://pib.sagepub.com/content/225/6/799>

Published by:



<http://www.sagepublications.com>

On behalf of:



[Institution of Mechanical Engineers](http://www.institutionofmechanicalengineers.org)

Additional services and information for *Proceedings of the Institution of Mechanical Engineers, Part B: Journal of Engineering Manufacture* can be found at:

Email Alerts: <http://pib.sagepub.com/cgi/alerts>

Subscriptions: <http://pib.sagepub.com/subscriptions>

Reprints: <http://www.sagepub.com/journalsReprints.nav>

Permissions: <http://www.sagepub.com/journalsPermissions.nav>

Citations: <http://pib.sagepub.com/content/225/6/799.refs.html>

>> [Version of Record](#) - Jul 21, 2011

[What is This?](#)

The influence of feed rate on process damping in milling: modelling and experiments

N D Sims^{1*} and M S Turner²

¹Department of Mechanical Engineering, University of Sheffield, Sheffield, UK

²Advanced Manufacturing Research Centre with Boeing, University of Sheffield, Advanced Manufacturing Park, Rotherham, UK

The manuscript was received on 30 April 2010 and was accepted after revision for publication on 22 July 2010.

DOI: 10.1243/09544054JEM2141

Abstract: The performance of milling operations is limited by the onset of unstable self-excited vibrations known as regenerative chatter. Over the past few decades there has been a great deal of research to help predict and explain regenerative chatter. Consequently, high-speed milling operations are now frequently employed, with judicious choice of spindle speeds and depths of cut so as to avoid chatter whilst maintaining high productivity. However, many materials that are increasingly used in aerospace components are difficult to machine at high spindle speeds because of their thermal properties. Examples include titanium and nickel alloys. For these materials, low-speed machining must be employed, and in this regime the role of regenerative chatter is less clearly understood due to the phenomenon of process damping.

In the present study, a time domain model of process damping is developed. This model is used to explore the relationship between cutting conditions and the amplitude of chatter vibrations. A qualitative agreement is found between experimental behaviour and the numerical model. In particular, the model predicts a strong relationship between the workpiece feed rate (expressed as a feed per tooth), and the acceptable chatter stability defined by the process damping wavelength. Further work is needed to properly calibrate some of the model parameters.

Keywords: milling chatter, process damping, time domain modelling, regenerative chatter

1 INTRODUCTION

It is well known that at low spindle speeds the stability of milling operations is enhanced by the phenomenon known as process damping. The concept of process damping was first conceived by Tobias and Fishwick [1], who argued that the rubbing between the flank face and just-cut surface resulted in forces that damped the self-excited vibration. Tlustý [2] illustrated this concept schematically as shown in Fig. 1. Here, it can be seen that there is a greater potential for tool/flank interference when the tool is

at location 'B' on the wavy surface. This results in a force that is out of phase with the vibration velocity, giving rise to a damping effect.

Despite this early contribution, research into milling chatter stability has largely focused on high-spindle-speed scenarios, and process damping remains one of the least-understood aspects of machining [3]. This is partly due to the prevalence of aluminium alloy components in the aerospace industries, which can be machined with high productivity by using high surface speeds. However, recent trends towards exotic materials such as titanium and nickel alloys have resulted in machining scenarios that cannot involve high spindle or surface speeds, due to the thermal and hardness characteristics of these materials. Consequently, there is now a greater

*Corresponding author: Department of Mechanical Engineering, University of Sheffield, Mappin St, Sheffield S1 3JD, UK.
email: n.sims@sheffield.ac.uk

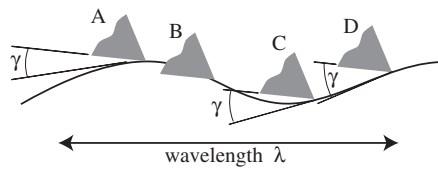


Fig. 1 Process damping during cutting. The effective relief angle γ changes depending on the tool's position relative to the wavy workpiece surface

need to understand and utilize the phenomenon of process damping in milling.

The present contribution aims to demonstrate the application of the conceptual model proposed by Tobias and Fishwick [1] to a time domain simulation of low radial immersion milling. A qualitative comparison is then made with a series of milling experiments that were performed under similar conditions to the model. It is shown that increasing the tool feed rate enhances the process damping effect in both the experiment and the simulation, and that the process-damped vibrations exhibit limit-cycle behaviour rather than the theoretical stability associated with non-process damped chatter-free cutting.

The remainder of this paper is organized as follows. First, relevant research on process damping in milling is briefly reviewed to justify the originality of the present contribution. Next, the time domain modelling procedure is explained in detail, before describing the experimental tests that were performed. Following a discussion, some conclusions are drawn and recommendations for further work are made.

2 LITERATURE REVIEW

Before considering research that has focused on process damping concepts, it is useful to briefly mention some of the recent developments concerning the modelling of stability prediction and analysis. Of particular relevance is the work of Mann *et al.* [4], who used techniques from non-linear dynamics (once-per-period sampling, and Poincaré sections) to analyse numerical and experimental data. The focus of their work, however, was the chatter vibrations that occur at very low radial immersions, rather than the behaviour at low spindle speeds. Other recent activity has also focused on the behaviour at low radial immersion: for example Insperger's semi-discretization approach [5–9]. This concept has more recently been extended to consider variable helix tools [10]

and runout [11]. The issue of tool runout was also considered by reference [12].

Previous investigations into process-damped machining have focused on various aspects. Since the present study focuses purely on milling, earlier work regarding process damping in turning (or other material removal processes) will not be considered. Furthermore, for the sake of brevity this section will be restricted to those studies that have included a significant modelling aspect.

Early work on the mechanics of chip formation used a complex coefficient to relate cutting force to instantaneous chip thickness [13, 14]. The real part of this coefficient accounted for the forces in phase with the instantaneous chip thickness, whereas the imaginary part accounted for the out-of-phase forces. Tlustý [15] attributed the process-damping (i.e. out-of-phase) forces to the flank interference and changing relief angle shown in Fig. 1. This figure is also useful for visualizing the so-called process-damping wavelength λ_c . Since chatter vibration is often assumed to be sinusoidal, the chatter frequency f_c can be related to the wavelength of vibrations λ by

$$\lambda = \frac{v}{f_c} \quad (1)$$

$$v = \pi D \frac{n}{60} \quad (2)$$

Here, v is the surface speed of the tool compared to the workpiece, n is the spindle speed, and D the tool diameter (in milling). At low spindle speeds, chatter stability becomes almost independent of the axial depth of cut. The corresponding wavelength λ is often referred to as the process-damping wavelength λ_c .

Whilst this earlier work was useful for illustrating conceptual mechanisms for process damping, more recent studies have resorted to time domain simulations so that non-linear effects can be properly investigated. Montgomery and Altintas [16] attempted to include process-damping forces in a model of milling. It seems that this model did not fully consider the surface waviness on the process damping forces, and more recent work by Campomanes and Altintas [17] has focused on developing advanced models of higher speed milling.

Wu [18, 19] developed a model of ploughing forces during milling, assuming a rounded tool and a sinusoidal chip thickness variation. Force predictions were presented but the analysis stopped short of assessing the effect of the ploughing forces on chatter and tool wear. Elbestawi *et al.* [20] modified this approach to consider a wear flat on the tool and investigate the chatter stability. They showed an increase in stability with increasing length of wear

flat, and some correlation between model and experiment at three selected spindle speeds. Endres *et al.* [21, 22] developed a model of the ploughing mechanism that assumed a rounded tool but, unlike Wu's method, performed numerical integration to calculate the flank penetration volume. They used an empirical method to determine the penetration depth, and investigated the effect of the rake angle and the chip thickness, but did not consider chatter stabilization effects.

One of the issues faced by Wu and Endres was that in assuming that the tool has a rounded edge (as may be the case in practice), there is no longer a finite tool tip that can be used to define the depth of cut and the flank penetration. Waldorf *et al.* [23] investigated this issue by comparing theoretical predictions from two ploughing models with experimental behaviour. They found that it is more appropriate to model the rounded tool tip with a stable built-up edge attached, so that the tool can be thought of as having a chamfer. However, this work did not consider the effect of flank penetration that may occur during chatter.

Ranganath *et al.* [24] implemented a similar numerical method to Endres, to calculate the interference volume for a sharp tool, thereby avoiding the problems when a rounded tool is considered. Their method incorporated the time domain milling model developed by Sutherland [25], which calculates the location of the tool centre at each simulation time step. The chip thickness calculation simplifies the geometry of the cutting kinematics, and so the approach is less accurate than that adopted by Campomanes and Altintas [17]. Although Ranganath's work used a numerical integration routine, no convergence study was mentioned, and in the corresponding thesis [26] the problems of simulating very flexible structures were resolved by including additional damping terms in the model. The study did not determine the process damping wavelength that is commonly used to indicate the low-speed stability region. Furthermore, the tests were performed using aluminium at spindle speeds of at least 1000 r/min, making the study less relevant to current problems involving low-speed machining of titanium alloys.

More recently Huang and Wang [27] proposed a semi-analytical model that considered the dynamically changing angles of the ploughing and shearing forces during cutting. A matrix of empirical coefficients was used to characterize the process-damping forces, which were assumed to be functions of the direction of relative motion between tool and workpiece. Rahnema *et al.* [28] developed a model specifically for micro-milling, where the spindle speeds

tend to be considerably higher and the feed rate considerably lower than in conventional milling.

To summarize, there have been a number of attempts to model the forces that occur during milling at low spindle speeds, based upon the original conceptual theory proposed over 50 years ago. Some of these models have focused on the forces arising due to physical interference between the tool and workpiece, whilst other work has investigated the consequence of a changing relief and rake angle on the dynamic cutting forces [27]. Perhaps the most comprehensive work involving the former method is that described in the PhD thesis of Ranganath (see Ranganath *et al.* [24]). The aim of the present study is to complement and extend Ranganath's approach, as follows:

- implement a workpiece/tool flank interference model based upon the surface discretization methodology proposed by Campomanes and Altintas [17] and implemented by Sims [29];
- following a convergence study, utilize the model at an appropriately small numerical time step to ensure stable and steady-state predictions of cutting forces and displacements;
- qualitatively compare the model predictions to experimental data involving the very-low-speed machining of a titanium alloy;
- compare the process damping wavelength predicted from both the model and the experiment.

In the next section, the milling model will be described.

3 MODEL FORMULATION

The model used in the present study is an extension of that described by Sims [29], and this modelling approach will now be summarized.

The model is formulated in a Simulink environment, and consists of three aspects: milling kinematics, milling forces, and system dynamics. The kinematics model begins by dividing the tool into n_t discrete axial slices or layers, and calculating the tool and workpiece geometry within each slice. Two coordinate systems are used: a radial coordinate based upon the centre of the tool with angles taken relative to the feed direction, and a Cartesian coordinate system based upon the workpiece feed direction. The relative displacement of the workpiece and tool (accounting for feed rate and vibration effects) are provided as inputs to the calculation. The basis of the computation is the manipulation of a set of arrays of Cartesian coordinates (one array for each tooth on each axial slice) that define the surface of

the workpiece that was produced by that tooth. The array length represents a complete revolution of the tooth; therefore with each tooth revolution the array values are overwritten, or updated. For each time step in the simulation, the following calculations are repeated for each tooth on each axial slice.

1. The position of the tooth is calculated based upon the current simulation time, and the spindle speed.
2. The workpiece surface array for the present tooth is updated.
3. The instantaneous chip thickness for the present tooth is calculated, based upon the current tooth position and the surface array for the preceding tooth.
4. The geometrical interference between the tool flank and just-cut surface is calculated.

The calculations required for step (3) can be described with reference to Fig. 2. At this instantaneous point in time, the chip thickness h_{lt} can be calculated based upon the current tooth position and the workpiece surface coordinates representing the surface from the previous tooth pass. This is demonstrated in more detail in Fig. 3, which shows the data points stored in the workpiece surface arrays for each tooth. The chip thickness is calculated based upon these surface arrays and the position of the tooth tip (Fig. 3(b)). The flank contact or interference between the just-cut surface and the current position of the tool is then determined based upon the relief angle γ (Fig. 3(c)). The maximum allowable contact length is the flank length l_{flank} . In the present study, the length of contact l_{lt} was used to calculate the cutting forces that arise due to process damping. Furthermore, the workpiece material that has been penetrated by the flank surface is assumed

to plastically deform so that it follows the flank surface.

Having calculated the chip thickness and workpiece/flank contact, the cutting forces are then calculated as follows. As with many previous publications, the cutting forces due to the mechanics of chip generation are given by

$$f_{rc_{lt}} = \frac{b}{n_l} (K_{rc} h_{lt} + K_{re})$$

$$f_{tc_{lt}} = \frac{b}{n_l} (K_{tc} h_{lt} + K_{te})$$
(3)

Here, b is the axial depth of cut and n_l is the number of axial layers used in the simulation. With reference to Fig. 2, $f_{rc_{lt}}$ is the cutting force due to the chip mechanics acting in the radial direction of the tooth, for layer l and tooth t . Likewise, $f_{tc_{lt}}$ is the cutting force due to the chip mechanics acting in the tangential direction of the tooth, for layer l and tooth t . The coefficients K_{rc} and K_{tc} are the widely used cutting force coefficients that must be empirically obtained for a particular workpiece and (often) a particular tool. The edge or rubbing force coefficients K_{re} and K_{te} are also included in the model formulation, but for simplicity they are initially assumed to be zero.

Meanwhile, in the present study the process damping forces are assumed to be given by

$$f_{np_{lt}} = K_{np} l_{lt} \frac{b}{n_l}$$

$$f_{fp_{lt}} = \mu K_{np} l_{lt} \frac{b}{n_l}$$
(4)

With reference to Fig. 2, $f_{np_{lt}}$ is the cutting force due to process damping, acting in the direction normal to

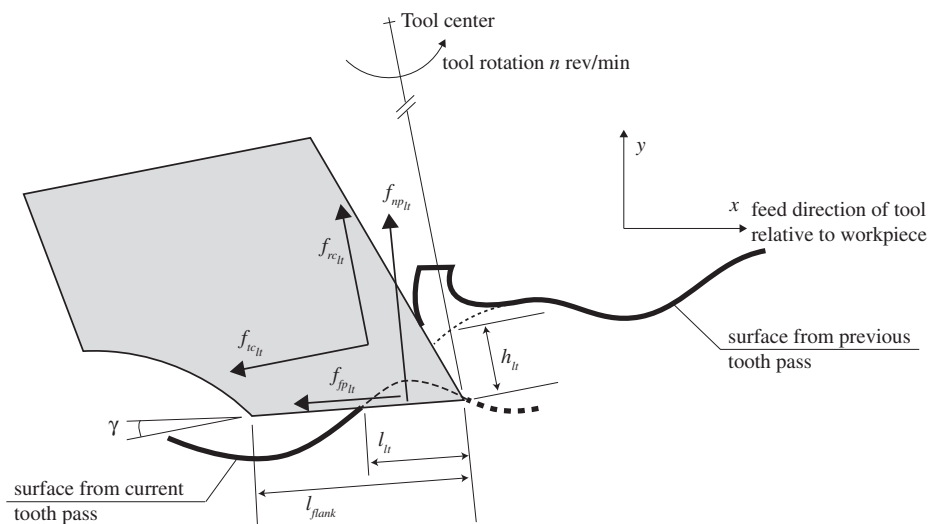


Fig. 2 Cutting force calculation for tooth t and axial slice l

the flank face, for layer l and tooth t . Meanwhile, $f_{fp_{lt}}$ is a friction force acting in a perpendicular direction. Equation (4) has introduced two new variables: the process damping normal force coefficient K_{np} , and a corresponding coefficient of friction μ .

It is straightforward to resolve the above-mentioned forces into components $f_{x_{lt}}$ and $f_{y_{lt}}$ acting in the x - and y -directions respectively. The total forces acting on the tool in the x - and y -directions can then be determined as

$$F_x = \sum_{l=1}^{n_l} \sum_{t=1}^{n_t} f_{x_{lt}} \quad (5)$$

$$F_y = \sum_{l=1}^{n_l} \sum_{t=1}^{n_t} f_{y_{lt}} \quad (6)$$

where n_t is the number of teeth on the tool. Note that during the calculation of the milling kinematics, teeth that are not engaged in the workpiece (due to their angular position, or due to the advent of severe chatter) have zero chip thickness and hence zero cutting force.

Having calculated the total forces acting on the tool, the corresponding displacement can be obtained by modelling the structural dynamics of the flexible tool. These displacements are then fed back to the milling kinematics model. The resulting Simulink model is shown in Fig. 4. Here, the cutting force calculation (Fig. 4(b)) is implemented as a subsystem of standard Simulink blocks, whereas the more complex kinematics model is implemented as a C program that interfaces with Simulink via the s-function/mex-file syntax [30]. With reference to Fig. 4(a), in the present study a

single mode of vibration was considered in the y -direction. In practice this can be readily extended to consider multiple degrees of freedom and coupled dynamics between the x - and y -directions.

Once the Simulink model was finalized, computational effort was reduced by compiling the model as a C program executable. This also enabled multiple simulation runs to be performed on a cluster of desktop PCs. Further details of this procedure are given in Sims *et al.* [31].

4 EXPERIMENTAL SETUP

A series of milling experiments were performed so that model results could be qualitatively compared with the experimental data. Experiments were performed on a Mori Seiki SV500 vertical machining centre, using a 16 mm diameter solid carbide tool with four teeth, a 6.6 degree rake angle, 6 degree relief angle, and 30 degree helix angle, to machine a titanium Ti-6-Al-4V workpiece. The experimental parameters are summarized in Table 1. Here, the maximum chip thickness h_{max} is a function of the feed per tooth f_b , radial immersion a_e , and tool diameter D , as follows

$$h_{max} = f_t \sqrt{\frac{4a_e}{D} - \left(\frac{2a_e}{D}\right)^2} \quad (7)$$

Low radial and high axial depths of cut were used to minimize damage in the event of severe chatter. During the experimental cut, the spindle speed was gradually increased in increments, whilst maintaining a constant feed per tooth. The tool vibration was

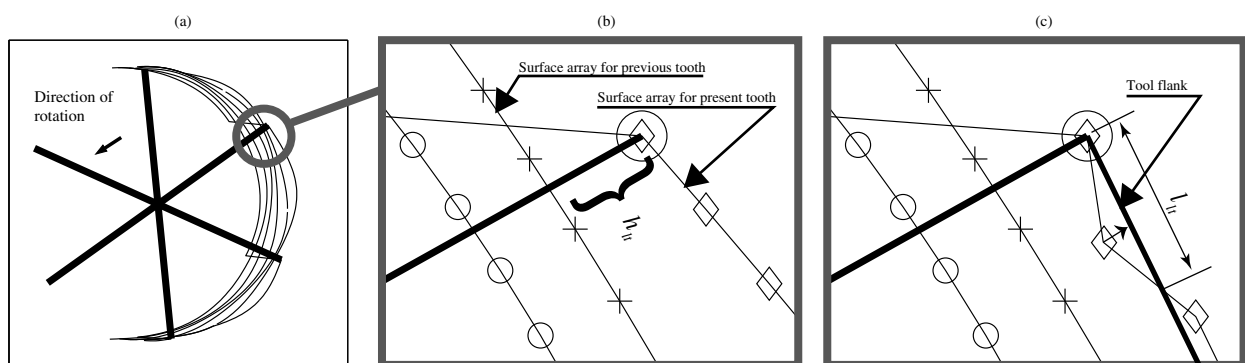


Fig. 3 Simulation of chip thickness for a tool with six teeth. Close-up (b) shows how the chip thickness h_{lt} is calculated based upon the intersection of two lines. One line is line from the present tooth's position to the tool centre, and the other line is the segment of the workpiece surface array for the previous tooth. Close-up (c) shows a scenario where tool flank/workpiece interference has occurred. The contact length l_{lt} is calculated from the intersection of two lines. One line represents the flank face of the tool, and the other line is the relevant segment of the workpiece surface array for the present tooth. If the workpiece is assumed to plastically deform, then any workpiece surface array elements within the interference zone are moved radially outwards as shown by the arrow

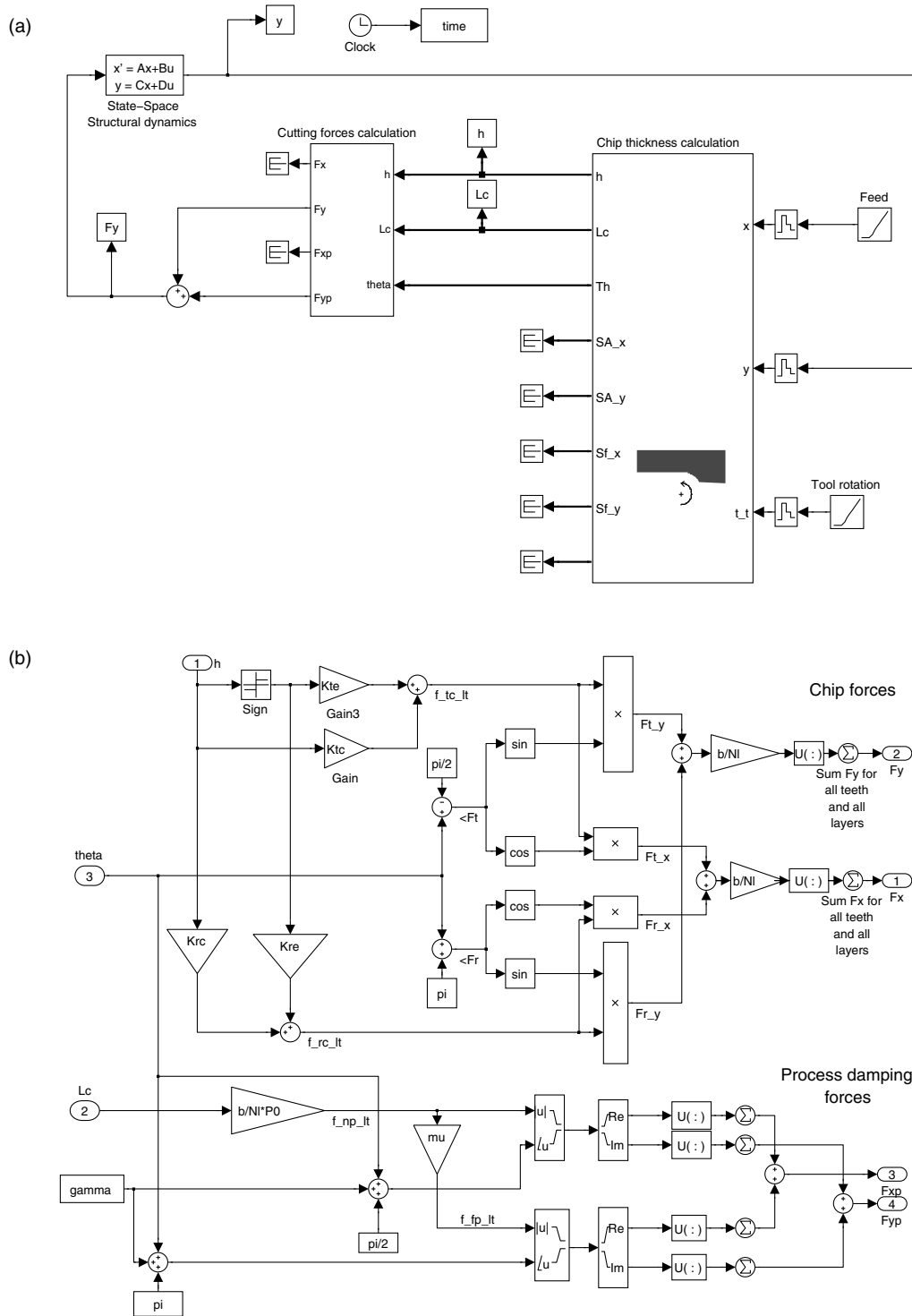


Fig. 4 Simulink model for process damped milling: (a) main simulink system; (b) ‘Cutting forces calculation’ subsystem. The ‘Chip thickness calculation’ subsystem is implemented as a C program with approximately 600 lines of code to calculate the chip thickness and contact length as illustrated in Fig. 3

Table 1 Experimental parameters

Parameter	Test 1	Test 2	Test 3	Test 4
Maximum chip thickness h_{max} (mm)	0.03	0.05	0.07	0.1
Radial immersion a_e (mm)	1	1	1	1
Axial depth of cut b (mm)	30	30	30	30

monitored using a microphone so that after the cut the spindle speed at which chatter occurred could be determined along with the corresponding chatter frequency f_c . From this the process damping wavelength could then be determined using equation (2) and equation (1). This procedure was then repeated for different values of maximum chip thickness h_{max} .

5 RESULTS

In this section, some typical simulation results are first presented to demonstrate model performance, justify some of the modelling parameter choices, and propose methods for analysing the simulation data. Then, comparisons are drawn between simulated and experimental data.

The simulation parameters are summarized in Table 2. It can be seen that the number of time steps per cycle or revolution of the tool is very high compared with previous studies on high-speed milling [29]. This is justified with reference to Fig. 5, which shows an example of the simulated tool and workpiece for one instance in time. It should be re-iterated that the data shown in Fig. 5 represent one tool and one axial slice in the simulation. Close inspection of Fig. 5 reveals that at this point in time the length of contact between the tool flank and workpiece is approximately $20\ \mu\text{m}$. With a tool diameter of 16 mm and 12000 time steps per tool revolution (Table 2), this contact length is represented by six discrete data points in the array of surface coordinates. Clearly the high number of time steps per revolution (or small step size) is needed to achieve an accurate representation of this contact region.

This small time step has a negative impact on the simulation's computation time. However, two other factors influence this computation time, namely the number of axial slices n_b , and the number of simulated revolutions. Using a high number of axial slices is important because this improves the accuracy with which the tool's flutes are represented. This has a significant effect on the amplitude of the forced vibrations, which become smoother as more axial slices are used. In the present study, 30 axial slices were used. Meanwhile, the 40 revolutions of the tool were used to ensure that the simulation had reached a steady-state condition. As a result each simulation took approximately 30 minutes to compute on a desktop PC.

In Fig. 6, the dynamic response of the model is illustrated by plotting the simulated tool displacement versus the simulated tool velocity (i.e. the phase trajectory). At a very low depth of cut (Fig. 6(a)), the phase trajectory indicates that with each cycle or revolution there are many oscillations of the tool. This is because the natural frequency of the tool (600 Hz) is

Table 2 Simulation parameters

Number of cycles (-)	40
Iterations per cycle (-)	12000
Number of axial layers n_l (-)	30
Radial cutting force coefficient K_{rc} (Nmm^{-2})	503
Tangential cutting force coefficient K_{tc} (Nmm^{-2})	1676
Radial cutting edge force coefficient K_{re} (Nmm^{-2})	0
Tangential cutting edge force coefficient K_{te} (Nmm^{-2})	0
Process damping friction coefficient μ (-)	0.25
Process damping normal force coefficient K_{np} (Nmm^{-2})	80
Number of teeth n_r (-)	4
Tool diameter D (mm)	16
Tooth flank length l_{flank} (mm)	0.3
Tool relief angle γ (deg)	5
Tool helix angle (deg)	30
Depth of cut b (mm)	30
Radial immersion a_e (mm)	1
y -direction natural frequency (Hz)	600
y -direction stiffness (MNm^{-1})	40
y -direction damping ratio (-)	0.01

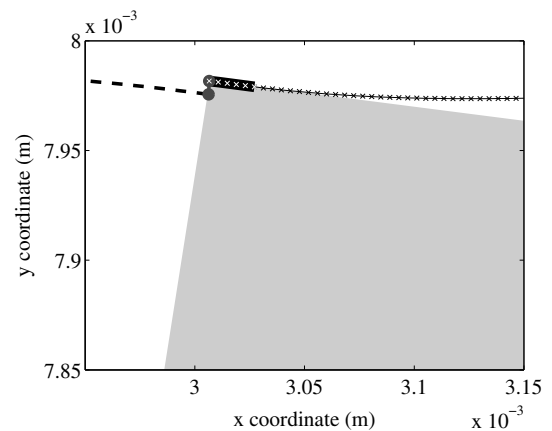


Fig. 5 Typical simulation output. The tool is rotating clockwise and the workpiece is located above the tool. - - - previous surface, — new surface, ■ contact region, ●-● chip thickness. 'x' markers indicate discrete coordinates representing the just-cut surface for the current tool

considerably higher than the spindle speed. Also shown in Fig. 6(a) are square markers corresponding to the vibration sampled at the tooth passing frequency (i.e. once per tooth samples). It can be seen that the markers are all superimposed, indicating that with each revolution of the tool the vibration has returned to its previous state. This represents a stable response from a non-linear dynamics perspective, or a chatter-free cut from a machining perspective.

Fig. 6(b) shows a quite different pattern of behaviour when the depth of cut is increased to 30 mm. Here, there are still a high number of tool oscillations per revolution, but the vibration magnitude is higher, and the once/tooth samples do not converge to one position. From a non-linear dynamics perspective,

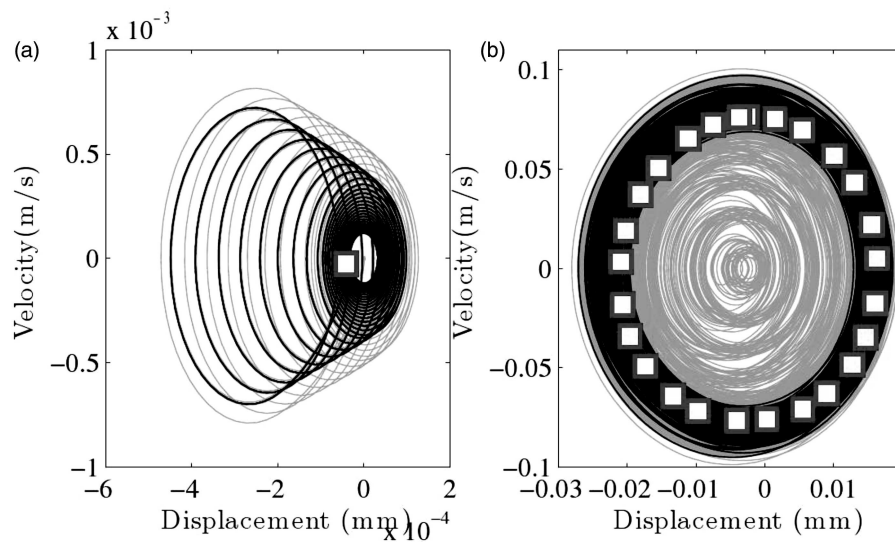


Fig. 6 Phase portrait at 326 r/min and maximum chip thickness of 0.03 mm. (a) 0.3 mm depth cut; (b) 30 mm depth cut. — Phase trajectory. — Phase trajectory, last cycle. □ Once/tooth samples – last 25 cycles

the system would be said to be unstable due to the occurrence of a Hopf bifurcation leading to quasi-periodic motion. However, from a practical machining perspective the magnitude of this ‘unstable’ behaviour may not be sufficient for it to be described as ‘chatter’. Consequently, the output from the numerical simulation is not straightforward to analyse in terms of chatter stability.

In the present study this issue is overcome using the following analysis procedure. First, the simulated displacement for the last tool revolution is de-trended to remove the DC component. Next, the root-mean-square value is obtained. This ‘AC r.m.s. vibration amplitude’ is a useful indicator of the vibration because:

1. it can readily distinguish between the low amplitude stable vibration shown in Fig. 6(a), and the limit cycle behaviour shown in Fig. 6(b);
2. it is insensitive to the DC or mean cutting forces/displacements which are modified by the maximum chip thickness;
3. it is a similar measure to the audio measurement used in the experimental procedure, but more amenable to automated processing; this is because it does not require the tooth passing frequency (and its harmonics) to be filtered out of the signal.

Before implementing this analysis approach, the influence of the modelled process damping mechanics on the amplitude of the response will be considered. Repeating the simulation shown in Fig. 6(b) *without* process damping effects caused a catastrophic failure of the simulation within the first

few revolutions. This is because the chatter vibration became so severe that its magnitude was greater than the surface speed of the tool, causing the array of surface coordinates to rotate in a clockwise direction (i.e. opposite to the tool rotation). The model relies upon interpolation between these data points, and they are assumed to proceed in a clockwise sense. Consequently the model fails. This failure is because the only non-linearity that inhibits linear instability (i.e. exponential and unbounded growth of vibration) is the tool loss of contact. Including process damping in the model provides an additional energy dissipation mechanism that limits the vibration amplitude. This is further illustrated in Fig. 7 which shows that the process-damping forces are always dissipative (i.e. opposing the velocity of the motion). This agrees with the original notion of process damping proposed in early work [1].

Having illustrated the role of process damping in limiting the magnitude of the machining vibrations, a range of machining parameters will now be investigated so as to generate simulated data under similar conditions to the machining experiments. The simulation was repeated for four different feed rates corresponding to maximum chip thicknesses of 30, 50, 75, and 100 μm (as for the experiments). For each feed rate, 140 simulations were performed for different spindle speeds between 210 and 500 r/min. This required approximately 12 days of computation time. For each simulated response the AC r.m.s. vibration level was calculated using the steps described above. The results are summarized in Fig. 8. Having accounted for the increased static

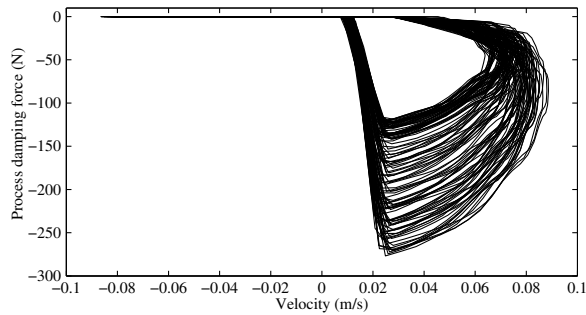


Fig. 7 Process-damping forces versus velocity for the example shown in Fig. 6(b)

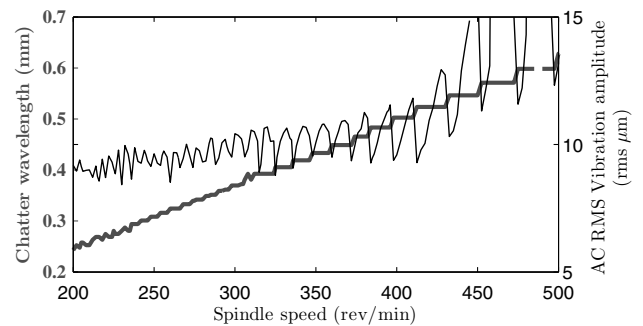


Fig. 9 Effect of spindle speed on vibration amplitude and chatter wavelength. $h_{max} = 75 \mu\text{m}$

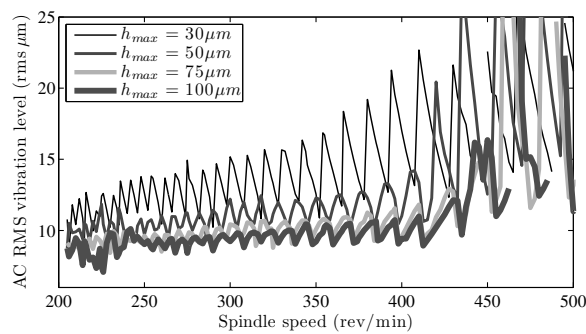


Fig. 8 Effect of spindle speed and feed rate on vibration amplitude

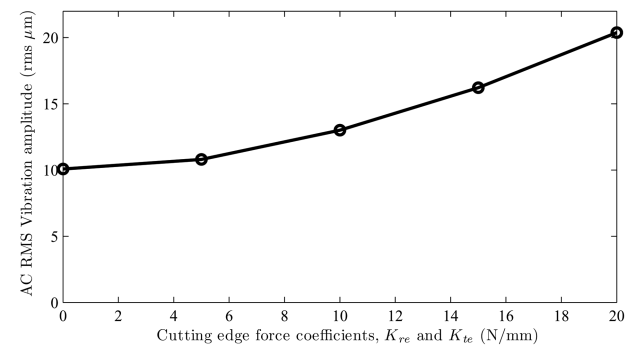


Fig. 10 Effect of cutting-edge force coefficients on vibration amplitude. Spindle speed 300 r/min, $h_{max} = 75 \mu\text{m}$

forces and deflections due to increasing the feed rate, it is clear that higher feed rates have actually resulted in a *reduction* in the response level. In other words, more process damping is achieved by increasing the feed per tooth or maximum chip thickness. A second interesting feature of Fig. 8 is that the vibration amplitude fluctuates in a seemingly erratic fashion as the spindle speed is changed.

This fluctuation is explained with reference to Fig. 9. Here, the data for $h_{max} = 75 \mu\text{m}$ are repeated (right-hand axis), with a calculation of the chatter vibration wavelength λ superimposed (left-hand axis). This calculation was performed by first obtaining the chatter frequency from a Fourier analysis of the last four tool revolutions, and then using equation (2) and equation (1) to determine λ . Fig. 9 shows that the chatter vibration wavelength increases in discrete steps as the spindle speed is increased. These steps coincide with the fluctuations observed in the vibration amplitude. Multiplying the reciprocal of the chatter wavelength by the circumferential distance between adjacent teeth on the tool ($\pi D/4$ for a tool with four teeth) gives the number of complete waves per tooth pass. In high-speed milling this is normally referred to as the 'lobe number'. For the data shown in Fig. 9, the lobe number varies

from approximately 50 (at 200 r/min) to approximately 25 (at 500 r/min). Consequently the fluctuations in vibration magnitude are all associated with constant lobe numbers, and so they are a result of the increasing phase difference between current and previous surface waves.

It should be pointed out that the preceding analysis has assumed that the cutting-edge force coefficients, K_{re} and K_{te} , are both zero. In practice these empirical coefficients could have a notable effect on the vibration amplitudes. This issue is explored in Fig. 10, where one simulation scenario is repeated for different values of the edge force coefficients (which are assumed to be equal to each other). It can be seen that the edge force coefficients do have a significant effect on the vibration amplitude, and so clearly they need to be properly calibrated in future work.

Having explained the main features of the model predictions, it is now appropriate to attempt to compare the model predictions with the experimental data. To recap, the experiments were performed by slowly incrementing the spindle speed – and hence the vibration wavelength – until the vibration magnitude exceeded a threshold value. For this situation,

the chatter vibration frequency was determined and the corresponding wavelength (the process-damping wavelength λ_c) calculated. The same procedure can be employed using the simulated data shown in Fig. 8. However, the experimental data used a threshold for a filtered audio signal measurement. Clearly this threshold cannot be used for the simulated data which uses a different analysis procedure. To overcome this issue, an arbitrary threshold of $12\ \mu\text{m}$ r.m.s. amplitude is chosen for the simulation data, and only a qualitative comparison is made with the experimental data. With reference to Fig. 9, the $12\ \mu\text{m}$ threshold is exceeded for spindle speeds greater than 425 r/min, corresponding to a chatter wavelength of 0.52 mm. This wavelength is therefore the process-damping wavelength for this value of maximum chip thickness. Repeating this procedure for the other values of maximum chip thickness leads to the results illustrated in Fig. 11.

6 DISCUSSION

The results that have been presented clearly show some promise in terms of the model's ability to represent experimentally observed behaviour. However, a number of issues are worthy of further discussion.

Most notably, it should be re-iterated that the process damping parameters used in the present study were neither formally calibrated, nor based directly upon underlying physical material properties. This clearly limits the applicability of the model results, and for this reason it should be re-iterated that only a qualitative comparison has been made with the experimental data. To make this comparison as fair

as possible, the remaining model parameters were chosen to match the experiments. For example, identical cutting scenarios were used (depth and width of cut, tool geometry, and empirical cutting force coefficients K_{rc} and K_{tc}). However, the cutting edge force coefficients, K_{re} and K_{te} were not comparable and a separate set of simulations has demonstrated that they have notable influence on the simulated vibration amplitude. Consequently they should be properly considered in future work. To aid the analysis of the model results, the model was constrained to only allow vibration in one direction (the y -direction), with a single mode of vibration. However, this mode of vibration was chosen to closely match the experimentally observed chatter frequency (around 600 Hz), which was associated with a mode of vibration of the machine's spindle [32].

The model parameters which were arbitrarily chosen were the process damping normal force coefficient K_{np} and the corresponding friction coefficient μ . In addition, the model assumed that the normal force was proportional to the flank/workpiece contact area (rather than contact volume), and that this material in contact was plastically deformed so that it followed the profile of the tool flank. In fact the model formulation is compatible with either volume- or area-based coefficients, and either plastic or elastic deformation of the contacting material. Further work is needed to develop informed values for these settings.

One possible approach to this would be to perform more detailed modelling of the chip mechanics (disregarding the self-excited vibration and other dynamic behaviour), using finite element techniques. This could indicate appropriate values for the process

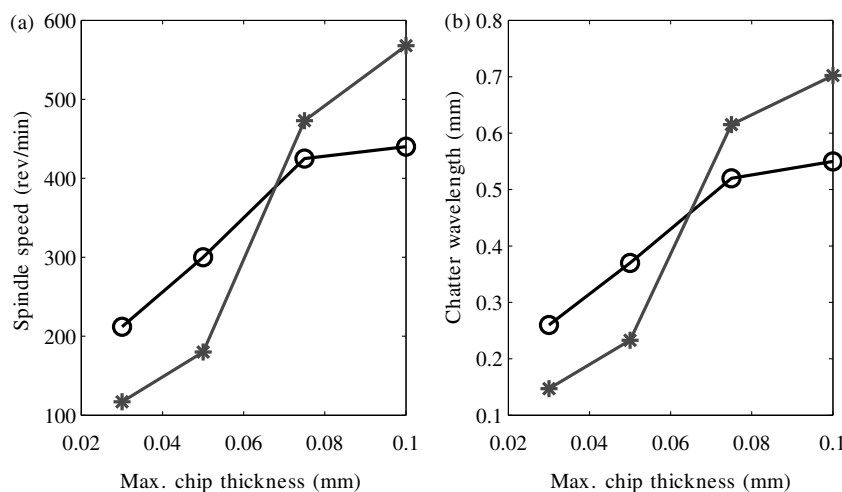


Fig. 11 Comparison between model predictions and experimental data. (a) Spindle speed at which process damping no longer suppresses chatter; (b) corresponding vibration wavelength. \circ model; * Experiment

damping force coefficients (as functions of volume or area). Such models would also indicate whether plastic or elastic deformation is the best assumption.

An alternative approach would be to configure and calibrate the model based upon empirical data from machining experiments. This procedure is already widely employed to choose the cutting force coefficients. However, calibration of the process-damping coefficients would be more complex due to the higher number of parameters and the difficulty of obtaining appropriate experimental data in the presence of measurement noise. For example, the process-damping forces depicted in Fig. 7 involve frequencies equal to the chatter frequency and its harmonics. These frequencies can be quite high in practice, making the forces more difficult to measure using a milling dynamometer. It is for these reasons that the present study has focused on illustrating that similar trends are observed in both the model and the experiment, instead of devoting effort to the calibration of the model parameters.

Another aspect of the model which requires attention is the consideration of tool geometry such as wear flats on the flank, and tool edge sharpness. Including these characteristics will certainly influence the contact region between the tool flank and the workpiece. In principle the model can be readily extended to include such geometrical features. However, this would also increase the complexity of the experimental calibration activity, since these aspects of tool geometry cannot be directly controlled during experimental machining.

Despite these issues, the overriding feature of the model is that it is able to predict similar trends to those observed experimentally: a strong relationship between feed per tooth and process damping wavelength.

7 CONCLUSIONS

The present study has described the implementation of a time domain model of milling chatter that considers process damping forces due to interference between the tool flank and the just-cut workpiece surface. The model predicts the following behaviour.

- At low spindle speeds, process-damping forces limit the amplitude of self-excited vibration arising due to regenerative chatter. The stability of the motion is not completely stabilized, but rather the resulting amplitude is sufficiently low for a corresponding experiment (in the presence of measurement noise and other unmodelled effects) to have been deemed 'stable'.
- The process damping forces are in phase with the velocity of the motion, leading to an energy dissipation mechanism as proposed by early research [1].
- The resulting motion is strongly influenced by the relative phase angle between current and previous workpiece surfaces.
- The amplitude of the motion rises substantially as the spindle speed is increased. This is in agreement with experimental observations under similar conditions.
- Using a threshold-based approach to defining the acceptable chatter stability, qualitatively similar behaviour was found in the model and experimental tests. In particular, it was shown that the process damping wavelength increased as the feed per tooth, or maximum chip thickness, was increased.

Finally, further work is needed to properly calibrate the model parameters based upon either empirical data or detailed modelling of the chip mechanics.

ACKNOWLEDGEMENT

The authors are grateful for the support of the EPSRC through grant reference EP/D052696/1.

© Authors 2011

REFERENCES

- 1 Tobias, S. A. and Fishwick, W. Theory of regenerative machine tool chatter. *The Engineer*, 1958, 199–203.
- 2 Tlustý, J. *Manufacturing processes and equipment*, 1999 (Prentice-Hall, Englewood Cliffs, New Jersey).
- 3 Altintas, Y. and Weck, M. Chatter stability of metal cutting and grinding. *CIRP Annals – Manuf. Technol.*, 2004, **53**(2), 619–642.
- 4 Mann, B. P., Bayly, P. V., Davies, M. A., and Halley, J. E. Limit cycles, bifurcations, and accuracy of the milling process. *J. Sound Vibr.*, 2004, **277**(1-2), 31–48. doi: dx.doi.org/10.1016/j.jsv.2003.08.040.
- 5 Insperger, T. and Stepan, G. Semi-discretization method for delayed systems. *Int. J. Numer. Methods Engng*, 2002, **55**(5), 503–518.
- 6 Mann, B. P., Insperger, T., Bayly, P. V., and Stepan, G. Stability of up-milling and down-milling, part 2: experimental verification. *Int. J. Mach. Tools Manuf.*, 2003, **43**(1), 35–40. doi: 10.1016/S0890-6955(02)00160-8.
- 7 Insperger, T., Mann, B. P., Stepan, G., and Bayly, P. V. Stability of up-milling and down-milling, part 1: alternative analytical methods. *Int. J. Mach. Tools Manuf.*, 2003, **43**(1), 25–34. doi: 10.1016/S0890-6955(02)00159-1.
- 8 Insperger, T. and Stepan, G. Updated semi-discretization method for periodic delay-differential equations with discrete delay. *Int. J. Numer. Methods Engng.*, 2004, **61**(1), 117.

- 9 **Inspurger, T.** Full-discretization and semi-discretization for milling stability prediction: Some comments. *Int. J. Mach. Tools Manuf.*, 2010, **50**(7), 658–662. doi: dx.doi.org/10.1016/j.ijmachtools.2010.03.010.
- 10 **Sims, N. D., Mann, B., and Huyanan, S.** Analytical prediction of chatter stability for variable pitch and variable helix milling tools. *J. Sound Vibr.*, 2008, **317**(3-5), 664–686. doi: 10.1016/j.jsv.2008.03.045.
- 11 **Wan, M., Zhang, W.-H., Dang, J.-W., and Yang, Y.** A unified stability prediction method for milling process with multiple delays. *Int. J. Mach. Tools Manuf.*, 2010, **50**(1), 29–41. doi: dx.doi.org/10.1016/j.ijmachtools.2009.09.009.
- 12 **Diez Cifuentes, E., Pérez García, H., Guzmán Villaseñor, M., and Vizán Idoipe, A.** Dynamic analysis of runout correction in milling. *Int. J. Mach. Tools Manuf.*, 2010, **50**(8), 709–717. ISSN 0890-6955. DOI: 10.1016/j.ijmachtools.2010.04.010.
- 13 **Das, M. K. and Tobias, S. A.** The relation between the static and the dynamic cutting of metals. *Mach. Tool Design Res.*, 1967, **7**, 63–89.
- 14 **Wallace, P. W. and Andrew, C.** Machining forces: some effects of removing a wavy surface. *J. Mech. Engng Sci.*, 1966, **8**(2), 129.
- 15 **Thusty, J.** Analysis of the state of research in cutting dynamics. *CIRP Annals*, 1978, **27**(2), 582–589.
- 16 **Montgomery, D. and Altintas, Y.** Mechanism of cutting force and surface generation in dynamic milling. *J. Engng Industry*, 1991, **113**, 160–168.
- 17 **Campomanes, M. L. and Altintas, Y.** An improved time domain simulation for dynamic milling at small radial immersions. *J. Manuf. Sci. Engng.*, 2003, **125**, 416–422.
- 18 **Wu, D. W.** Application of a comprehensive dynamic cutting force model to orthogonal wave-generating processes. *Int. J. Mech. Sci.*, 1988, **30**(8), 581–600.
- 19 **Wu, D. W.** A new approach of formulating the transfer function for dynamic cutting processes. *J. Engng Industry*, 1989, **111**, 37–47.
- 20 **Elbestawi, M. A., Ismail, F., Du, R., and Ullagaddi, B. C.** Modelling machining dynamics including damping in the tool-workpiece interface. *J. Engng Industry, Trans. ASME*, 1994, **116**(4), 435–439.
- 21 **Endres, W. J., DeVor, R. E., and Kapoor, S. G.** Dual-mechanism approach to the prediction of machining forces. Part 1: Model development. *J. Engng Industry*, 1995, **117**(4), 526–533.
- 22 **Endres, W. J., DeVor, R. E., and Kapoor, S. G.** Dual-mechanism approach to the prediction of machining forces. Part 2: Calibration and validation. *J. Engng Industry*, 1995, **117**(4), 534–541.
- 23 **Waldorf, D. J., DeVor, R. E., and Kapoor, S. G.** An evaluation of ploughing models for orthogonal machining. *J. Manuf. Sci. Engng.*, 1999, **121**, 550–558.
- 24 **Ranganath, S., Narayanan, K., and Sutherland, J. W.** The role of flank face interference in improving the accuracy of dynamic force predictions in peripheral milling. *J. Manuf. Sci. Engng.*, 1999, **121**(4), 593–599.
- 25 **Sutherland, J. W.** A dynamic model of the cutting force system in the end milling process. In *Sensors and Controls for Manufacturing*, PED-Vol. 33, 1988, pp. 53–62.
- 26 **Ranganath, S.** *A comprehensive model for dynamic force prediction in peripheral milling including the effects of flank face interference.* PhD Thesis, Department of Mechanical Engineering and Engineering Mechanics, Michigan Technological University, 1999.
- 27 **Huang, C. Y. and Wang, J. J. J.** Mechanistic modeling of process damping in peripheral milling. *J. Manuf. Sci. Engng, Trans. ASME*, 2007, **129**(1), 12–20.
- 28 **Rahnama, R., Sajjadi, M., and Park, S. S.** Chatter suppression in micro end milling with process damping. *J. Mater. Process. Technol.*, 2009, **209**(17), 5766–5776.
- 29 **Sims, N. D.** The self-excitation damping ratio: a chatter criterion for time-domain milling simulations. *J. Manuf. Sci. Engng*, 2005, **127**(3), 433–445.
- 30 **Matlab** Writing s-functions. 2004.
- 31 **Sims, N. D., Turner, M. S., and Ridgway, K.** A model of milling dynamics using Matlab and Simulink. In *Proceedings of the 9th CIRP International Workshop on modeling of machining operations* (Eds I. Grabec and E. Govekar), 2006 (University of Ljubljana, Bled, Slovenia).
- 32 **Turner, S.** *Titanium milling strategies.* PhD Thesis, Department of Mechanical Engineering, 2008.